Electronic Supplementary Material (ESI) for New Journal of Chemistry.

Supporting Informations

Enhancing effect of metal-nitrogen-carbon nanotubes with cobalt phthalocyanine on electrochemical reduction of CO_2

Ming Li [a, b], Hong-Lin Zhu [b], Xiao-fei Wang [b], Zhong-Yi Li [b], Jing-Jing Ma [b], Ya-Jun Guo [b], Yue-Qing Zheng* [b]

[a] China Certification & Inspection Group Ningbo Co., Ltd, Ningbo, Zhejiang, 315048, P. R. China

[b] Chemistry Institute for Synthesis and Green Application, School of Material Science and Chemical Engineering, Ningbo University, Ningbo, 315211, P. R. China

[c] ZhiEn Middle School of Ninghai, Ningbo, 315699, , P. R. China

*Corresponding author: Yue-Qing Zheng

E-mail address: zhengyueqing@nbu.edu.cn

1. Characterization

The Powder X-ray diffraction was carried out with a Bruker D8 Focus X-ray diffractometer with Cu-Kα radiation (λ = 1.54178 Å). Scanning Electron Microscope (SEM) was performed by using a Hitachi"s new SU-70 type of thermal field emission instruments. The low and high resolution transmission electron microscopy (TEM) and the corresponding energy dispersive spectroscope mapping analyses were performed on JME-2100. The X-ray photoelectron spectroscopy (XPS) was obtained on Escalab 250Xi instrument with a monochromatic Al Kα X-ray radiation source. The content of metal ions was determined by inductively coupled plasma optical emission spectrometer (ICAP 7200 ICP-OES). The liquid products were performed by Bruker 400 HZ NMR spectroscopy with TMS as an internal standard. The content of CO was analyzed by gas chromatograph (GC-2060) with flame ionization detector (FID).

2. Evaluation of Electrochemical Reduction CO_2

The working electrode was prepared by drop-drying method with 5 mg catalysts in a solution containing 120 μL Nafion solution, 400 μL isopropanol alcohol and 600 μL water. The suspension was sonicated for 30 min to obtain a homogeneous catalyst ink. Finally, 70 μL of catalyst ink were drop casted onto 1 × 0.5 cm^2 carbon cloth (loading: 0.3 mg cm^{-2}). The electrochemical measurements were carried out with three-electrode system in 0.5 M $KHCO_3$ solution on CHI 760E electrochemical workstation (ChenHua, Shanghai). A platinum sheet and Ag/AgCl electrode (saturated KCl) were used as a counter electrode and the reference electrode, respectively. All the measured potentials vs. Ag/AgCl were converted to reversible hydrogen electrode (RHE): $E_{RHE} = E_{Ag/AgCl} + 0.059 \times pH + 0.197$ V. The value of faradaic efficiency (FE) was calculated according to the formula: $FE = 2F \times n_{CO} / Q = 2F \times n_{CO} / (I \times t)$, where F is 96485 C/mol and n_{CO} is the molar

mass of CO. The TOF value of the electrocatalyst *via* mass loading was calculated as follows: $TOF(s^{-1}) = \frac{I \cdot FE/2F}{m \cdot \omega / M_r}$. The ECSA was calculated by the electrochemical double-layer capacitance (C_{dl}) with the cyclic voltammetry (CV) curves in non-faradaic potential region.

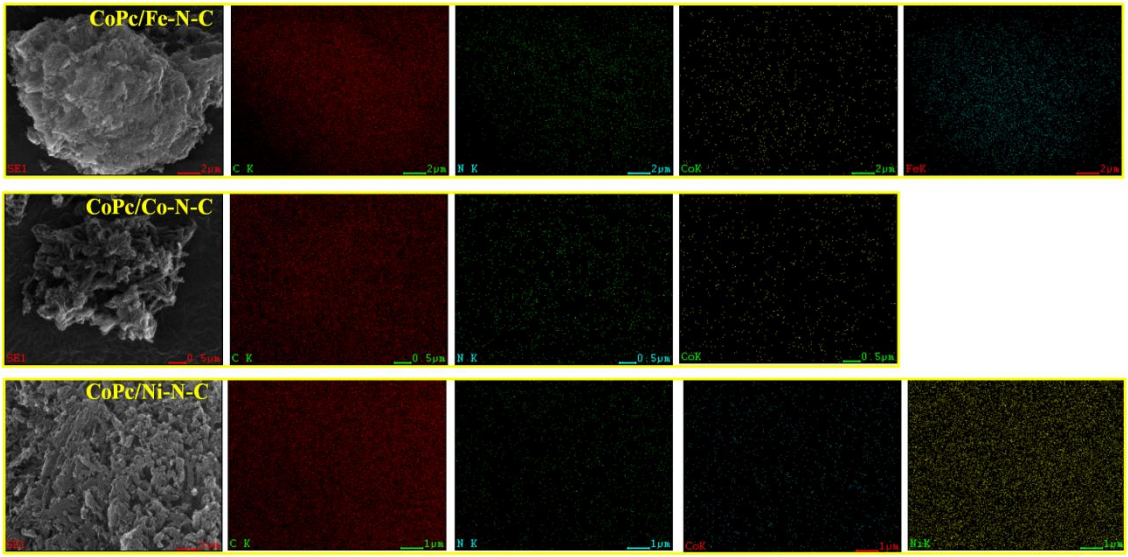

Figure S1. Element mapping of CoPc/M-N-C.

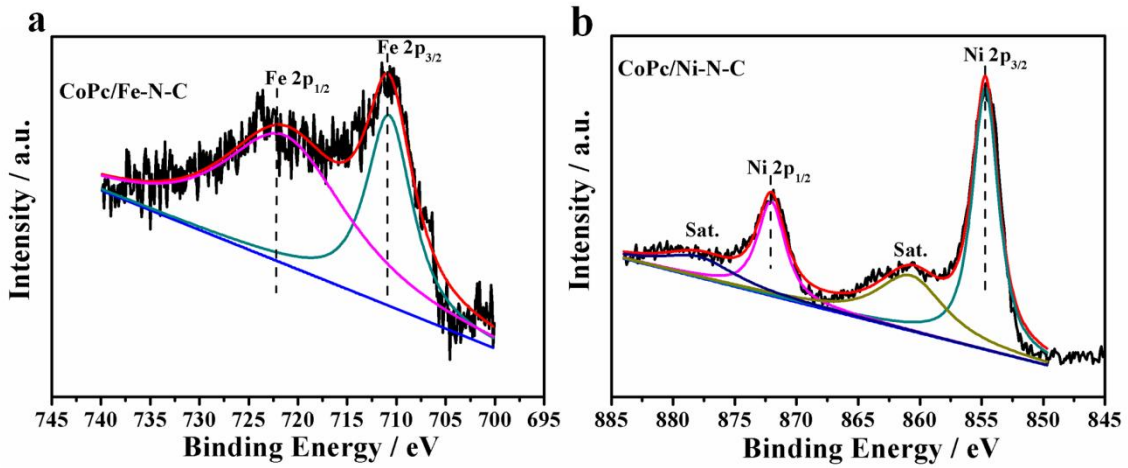

Figure S2. (a) Fe 2p and (b) Ni 2p high resolution XPS spectra of catalysts.

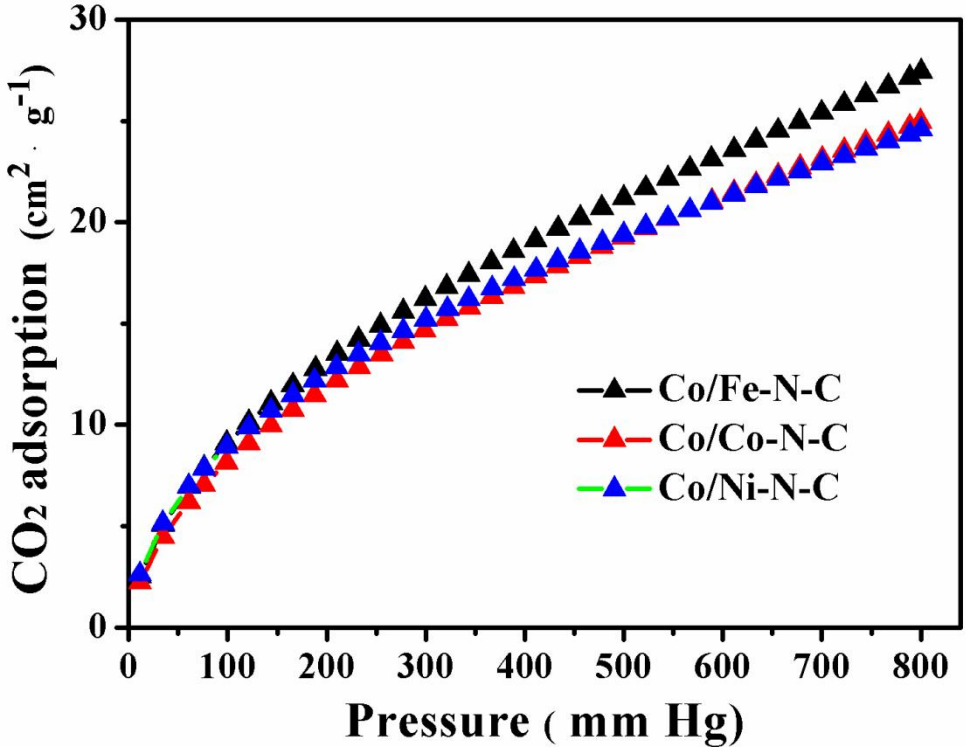

Figure S3. CO_2 adsortpion isotherms of CoPc/M-N-C.

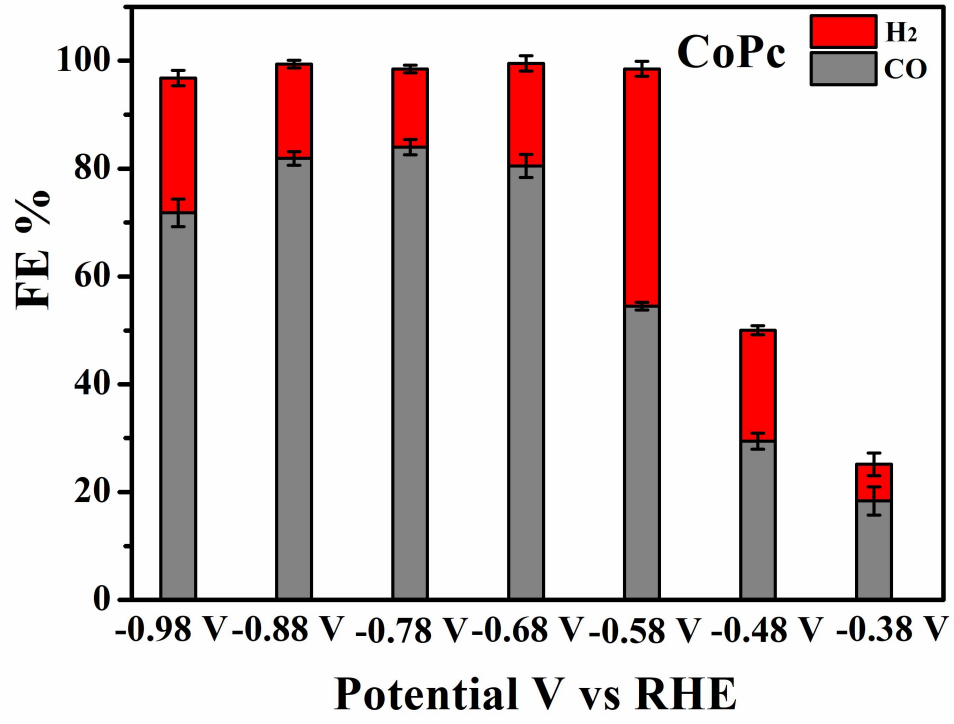

Figure S4 Faradic efficiency of CoPc

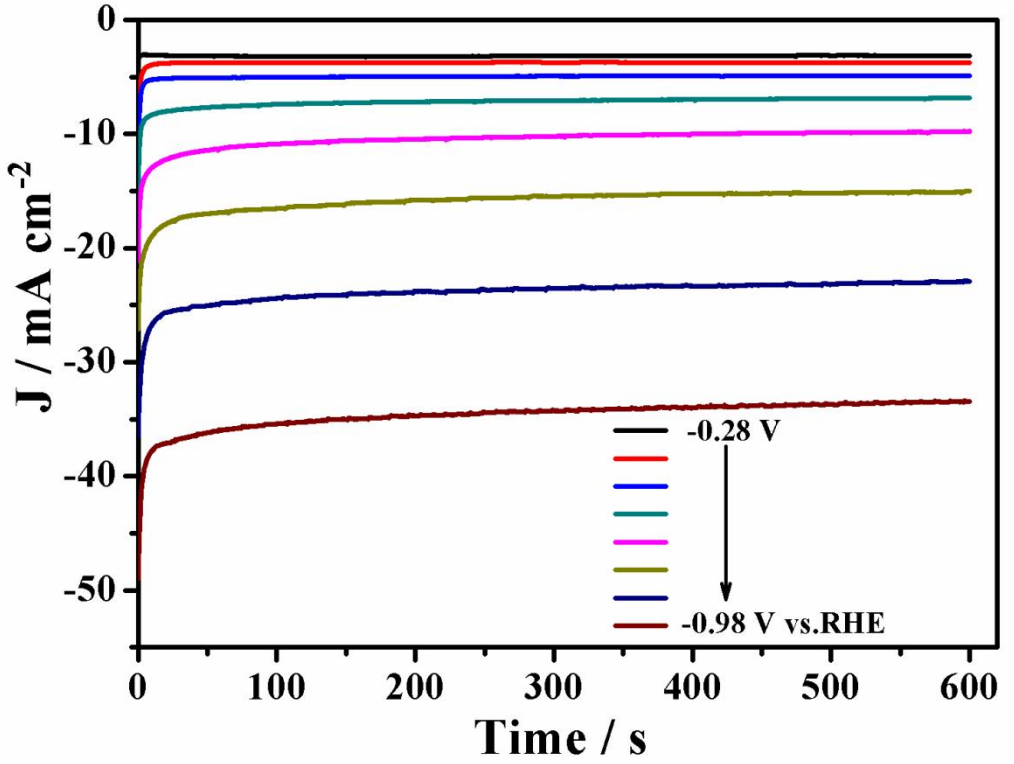

Figure S5. Current densities for CoPc/Fe-N-C at various potential.

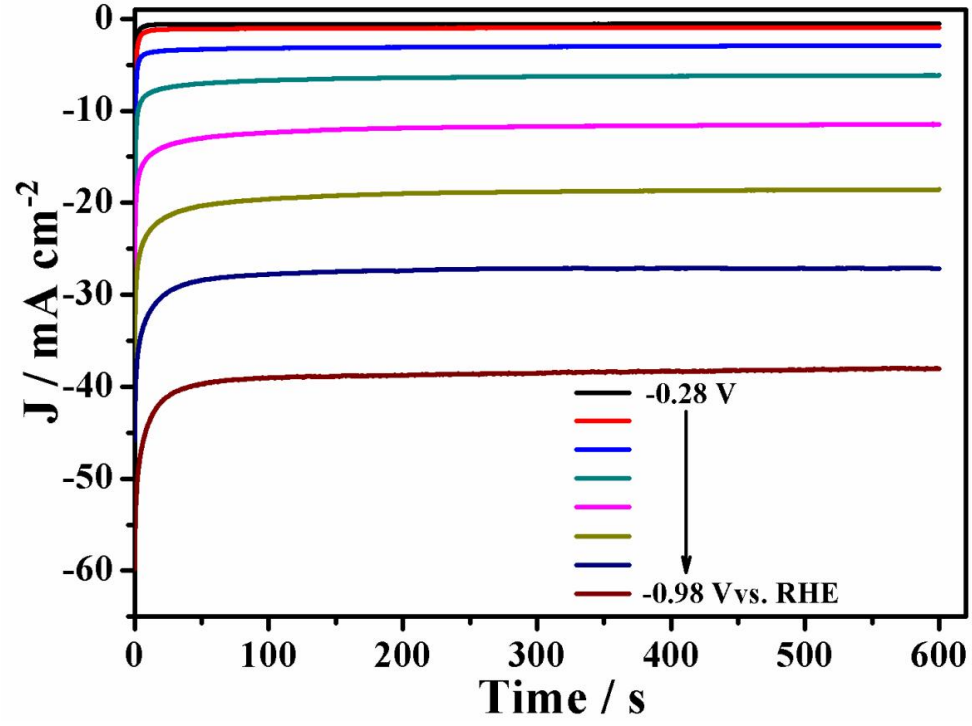

Figure S6. Current densities for CoPc/Co-N-C at various potential.

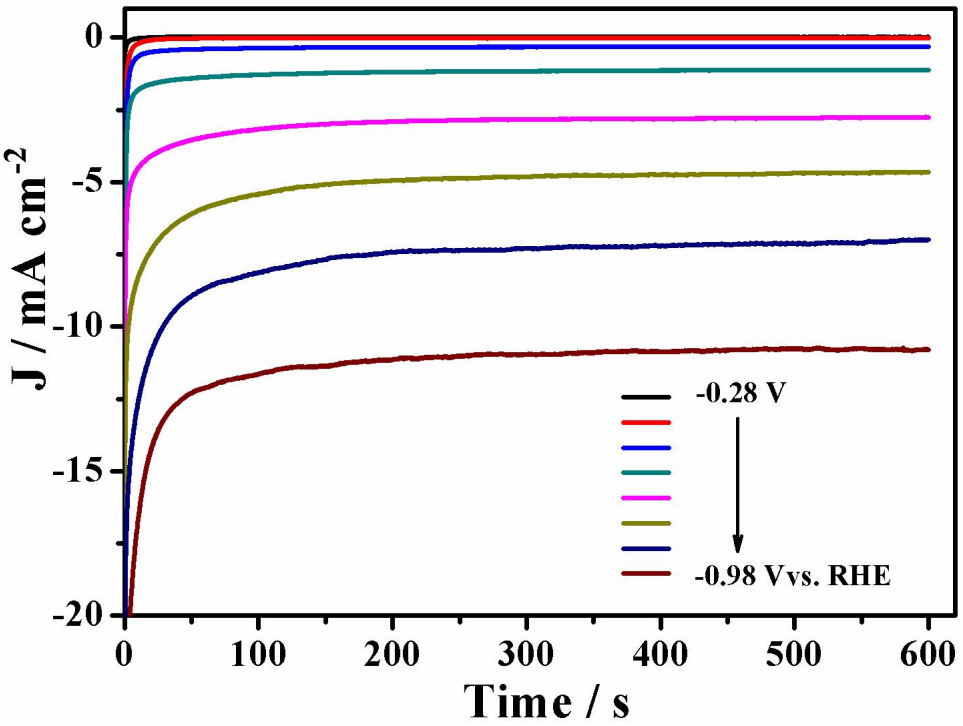

Figure S7. Current densities for CoPc/Ni-N-C at various potential.

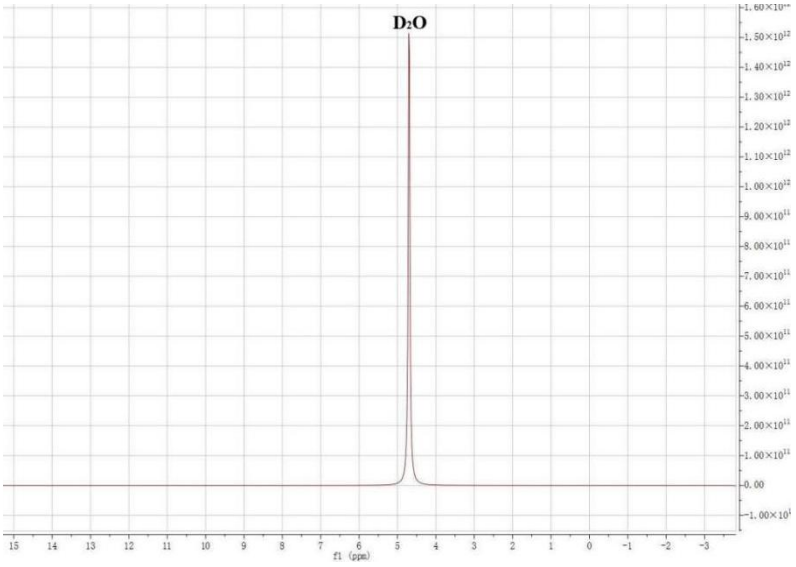

Figure S8. Liquid NMR spectrum at −0.68 V vs.RHE for CoPc/Fe-N-C.

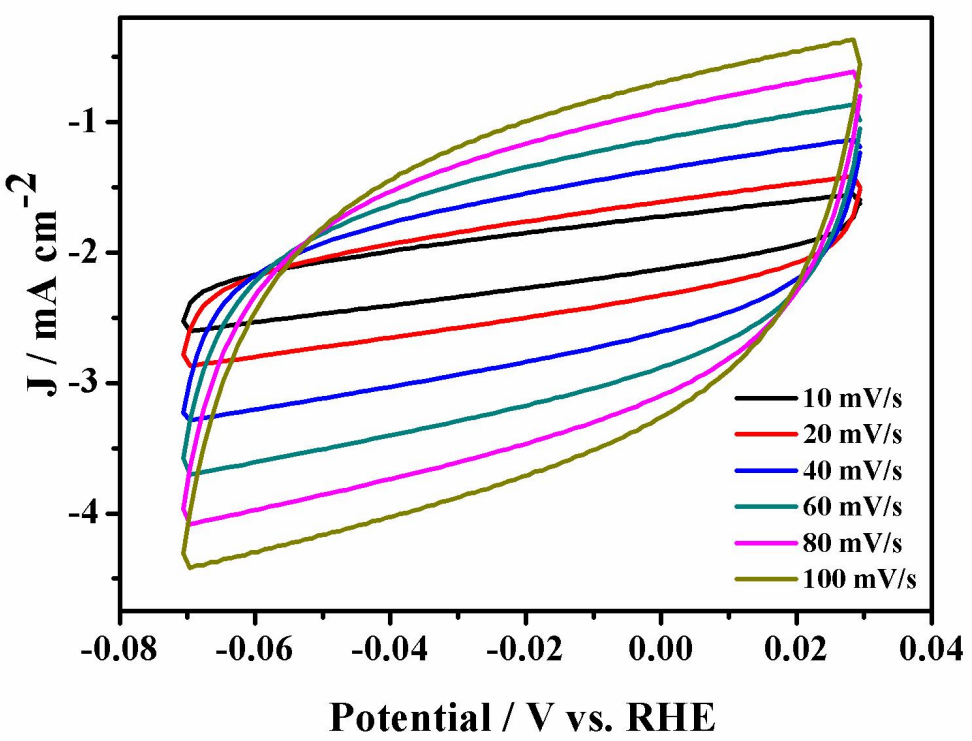

Figure S9. CVs plots in the non-faradaic potential for CoPc/Fe-N-C.

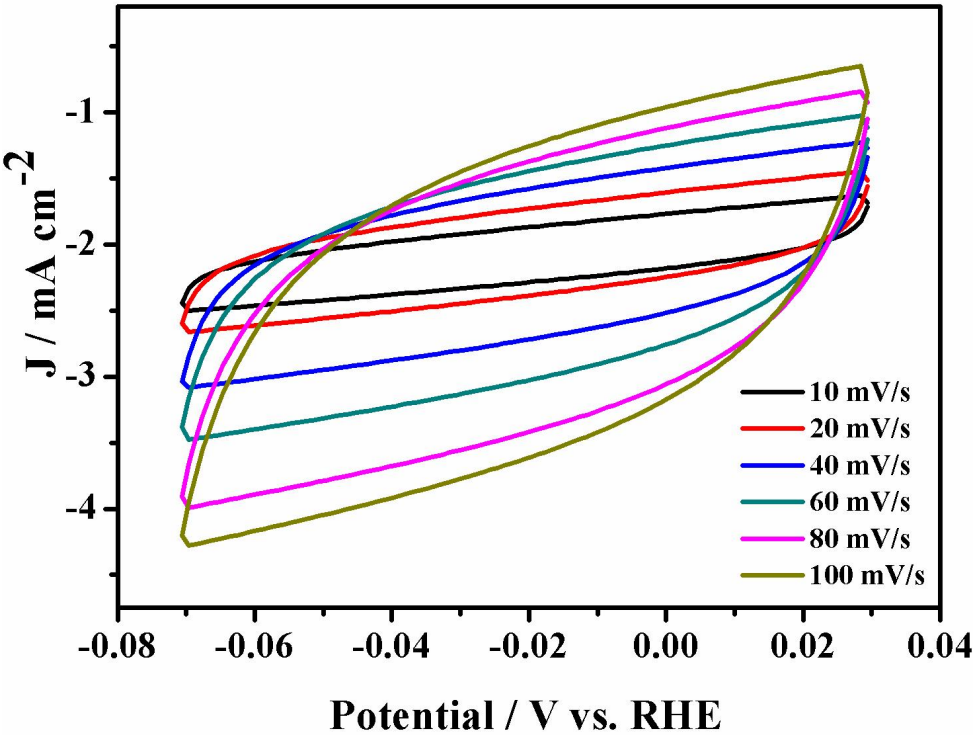

Figure S10. CVs plots in the non-faradaic potential for CoPc/Co-N-C.

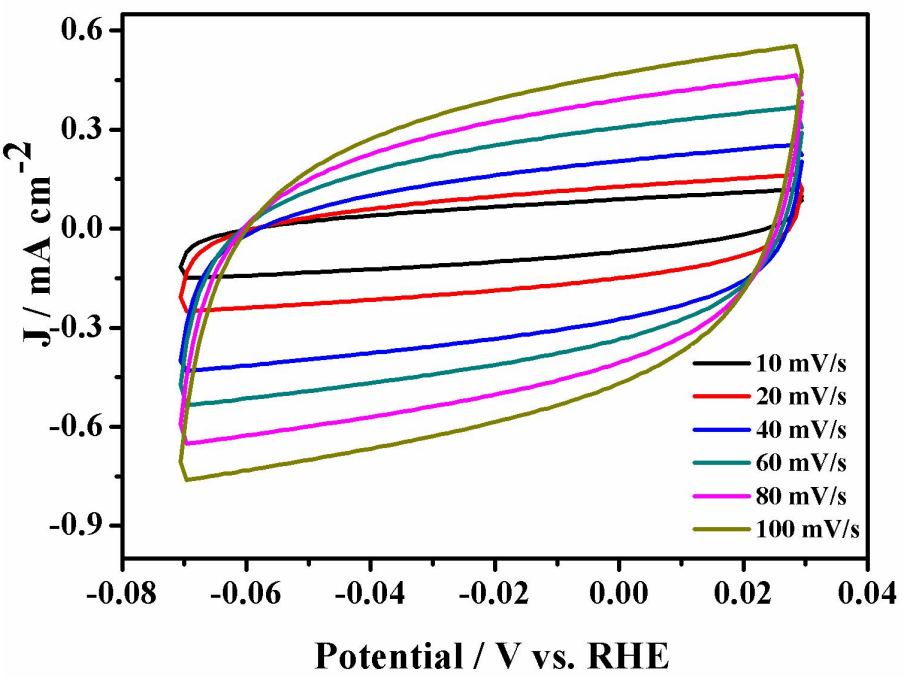

Figure S11. CVs plots in the non-faradaic potential for CoPc/Ni-N-C.

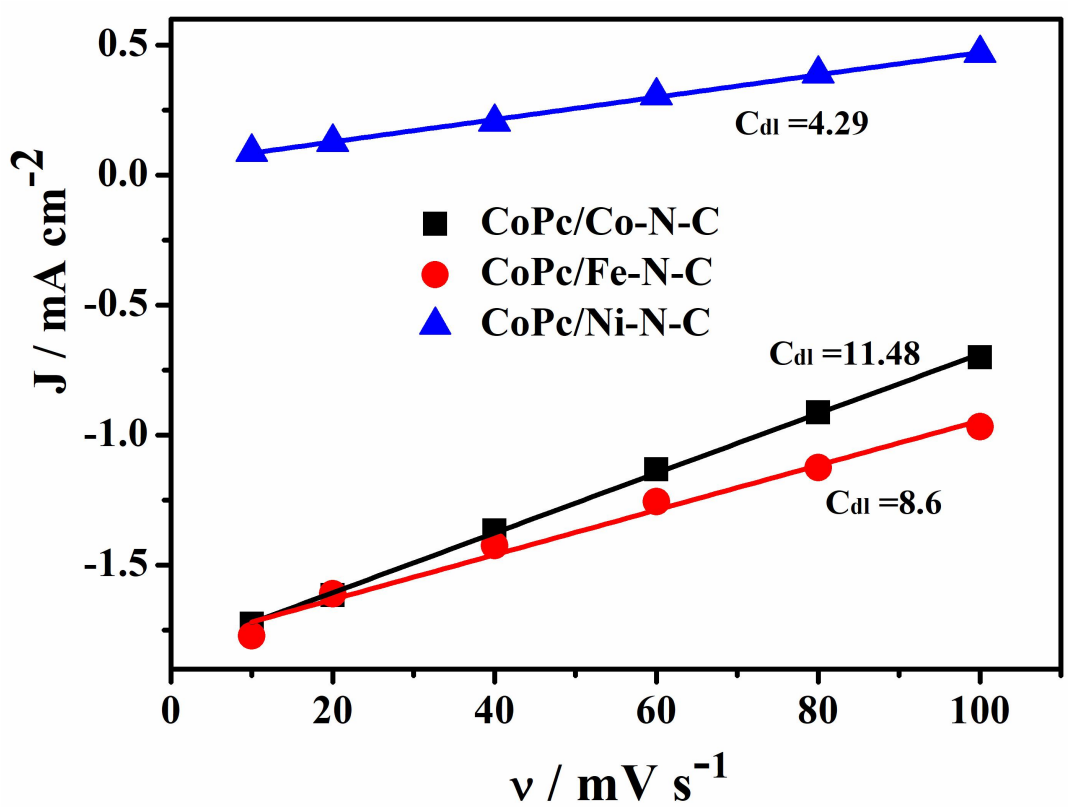

Figure S12. Current densities against the scan rates of CoPc/M-N-C.

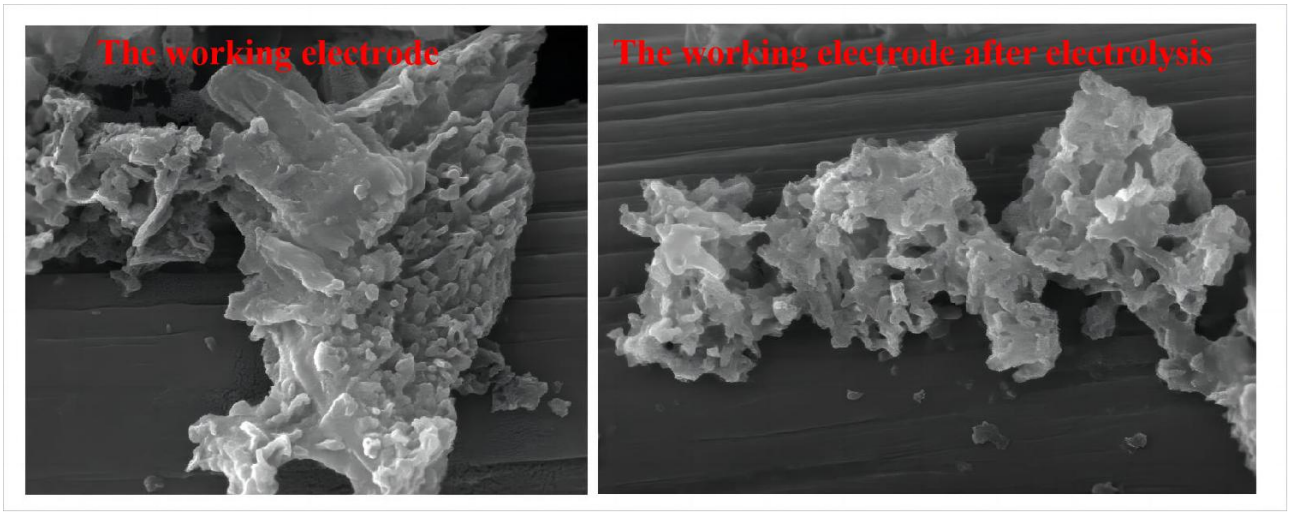

Figure S13.The SEM image of CoPc/Ni-N-C ink on carbon cloth

Table S1 ICP-OES results of transition metal loading amount.

Catalysts	Co (wt%)	Fe (wt%)	Ni (wt%)
CoPc/Fe-N-C	0.092	0.118	
CoPc/Co-N-C	0.230		
CoPc/Ni-N-C	0.182		0.075

Table S2 Porous properties of CoPc/M-N-C

Catalysts	$S_{Langmuir}$ (m^2 g^{-1})	V_p (cm^3 g^{-1})	Pore width (nm)
CoPc/Fe-N-C	97.16	0.0476	4.27
CoPc/Co-N-C	89.00	0.0433	4.31
CoPc/Ni-N-C	87.34	0.0429	4.05

Table S3 Summary of electrocatalytic CO_2RR with CoPc based catalysts reported in the literature

Catalysts	Load (mg/cm^2)	Product	On-set Potentials (V vs. RHE)	Faradaic efficiency		TOF (S^{-1})	Tafel slope (mV/dec)	Ref.
				Potentials (V vs. RHE)	FEco			
CoPc-P4VP	-	CO, H_2	-0.48	-0.73	>90%	4.8 (-0.73 V)	-	1
CoPc-A/CCG	0.12	CO, H_2	-0.49	-0.79	91.5%	5.0 (-0.6 V)	172	2
CoPc-py-CNT	-	CO, H2	-0.40	-0.53	91%	34.5 (-0.63 V)	117	3
CoPc/$ZnIn_2S_4$	0.50	CO, H_2	-	-0.73	93%	-	141	4
CoPc/CNT	0.40	CO, H_2	-0.46	-0.63	92%	2.7 (-0.63 V)	-	5
CoPc-CN/CNT	0.40	CO, H_2	-0.46	-0.63	98%	4.1 (-0.63 V)	-	5
CoPc/CNT-2	0.40	CO, H2	-0.40	-0.60	>90%	2.2 (-0.61 V)	-	6
CoPc/C	0.30	CO, H_2	-0.30	-0.60	>90%	3.9 (-0.70 V)	178	7
Co-N_5/HNPCSs	-	CO, H_2	-0.37	-0.57	>90%	0.14 (-0.70 V)	-	8
CoPc©Fe-N-C	-	CO, H_2	-0.13	-0.23	>90%	-	-	9
U_{120}-CoPc/KB	0.30	CO, H_2	-0.2	-0.7	96.4%	-	118	10
CoPc/Fe-N-C	0.30	CO, H_2	-0.28	-0.48	99%	6.33 (-0.48 V)	142	This study
CoPc/Ni-N-C	0.30	CO, H_2	-0.28	-0.58	>90%	1.15 (-0.48 V)	146	This study
CoPc/Co-N-C	0.30	CO, H_2	-0.28	-0.68	74%	1.26 (-0.48 V)	189	This study

Reference

1. W. W. Kramer, C. C. L. McCrory. Polymer coordination promotes selective CO_2 reduction by cobalt phthalocyanine. *Chem. Sci.*, 2016, **7**, 2506 2515.
2. J. Choi, P. Wagner, S. Gambhir, R. Jalili, D. R. MacFarlane, G. G. Wallace, D. L. Officer. Steric modification of a cobalt phthalocyanine/graphene catalyst to give enhanced and stable electrochemical CO_2 reduction to CO, *ACS Energy Lett.*, 2019, **4**, 666-672.
3. M. Zhu, J. Chen, R. Guo, J. Xu, X. Fang, Y. Han. Cobalt phthalocyanine coordinated to pyridine-functionalized carbon nanotubes with enhanced CO_2 electroreduction, *Appl. Catal. B Environ.*, 2019, **251**, 112−118.
4. C. Chen, X. Sun, D. Yang, L. Lu, H. Wu, L. Zheng, P. An, J. Zhang, B. Han. Enhanced CO_2 electroreduction via interaction of dangling S bonds and Co sites in cobalt

phthalocyanine/$ZnIn_2S_4$ hybrids, *Chem. Sci.*, 2019, **10**, 1659−1663.

5. X. Zhang, Z. Wu, X. Zhang, L. Li, Y. Li, H. Xu, X. Li, X. Yu, Z. Zhang, Y. Liang, H. Wang. Highly selective and active CO2 reduction electrocatalysts based on cobalt phthalocyanine/carbon nanotube hybrid structures, Nat. Commun., 2017, 8, 14675.
6. Z. Jiang, Y. Wang, X. Zhang, H. Zheng, X. Wang, Y. Liang, Revealing the hidden performance of metal phthalocyanines for CO_2 reduction electrocatalysis by hybridization with carbon nanotubes, *Nano Res.*, 2019, **12**, 2330–2334.
7. J. Ma, H. Zhu, Y. Zheng, M. Shui, An insight into anchoring of cobalt phthalocyanines onto carbon: Efficiency of the CO_2 reduction reaction, *ACS Appl. Energy Mater.*, 2021, **4**, 1442-1448.
8. Y. Pan, R. Lin, Y. Chen, S. Liu, W. Zhu, X. Cao, W. Chen, K. Wu, W. Cheong, Y. Wang, L. Zheng, J. Luo, Y. Lin, Y. Liu, C. Liu, J. Li, Q. Lu, X. Chen, D. Wang, Q. Peng, C. Chen, Y. Li. Design of single-atom $Co−N_5$ catalytic site: A robust electrocatalyst for CO_2 reduction with nearly 100% CO selectivity and remarkable stability, *J. Am. Chem. Soc.*, 2018, **140**, 4218-4221.
9. L. Lin, H. Li, C. Yan, H. Li, R. Si, M. Li, J. Xiao, G. Wang, X. Bao. Synergistic catalysis over iron-nitrogen sites anchored with cobalt phthalocyanine for efficient CO_2 electroreduction, *Adv. Mater.*, 2019, 1903470.
10. H. Zhu, L. Zhang, M. Shui, Z. Li, J. Ma, Y. Zheng, A novel manner of anchoring cobalt phthalocyanine on edge defected carbon for highly electrocatalytic CO_2 reduction, *J. Phys. Chem. Lett.*, 2023, **14**, 3844−3852